Proceedings of the 20th International Conference on Soil Mechanics and Geotechnical Engineering– Rahman and Jaksa (Eds)

Physical modelling of submarine debris flows: effects of bed conditions

Modélisation physique des flux de débris sous-marins: effets des conditions de lit

Jiantao Yu, Jianting Du & Clarence Edward Choi
Department of Civil Engineering, The University of Hong Kong, HKSAR, China, u3007330@connect.hku.hk

ABSTRACT: Submarine debris flows have been reported to cause severe damage to offshore infrastructure, including cables, pipelines, and platforms. Compared to their subaerial counterparts, submarine debris flows are typically several orders of magnitude larger in scale and travel a longer runout distance. Submarine debris flows are often modelled experimentally on rigid and impervious beds. However, in reality sea beds are mobile and pervious. Such bed conditions influence the momentum exchange between the flow and bed via enhanced friction stresses, drainage at the flow-bed interface, and mass exchange. In this study, a new submarine debris flow model was developed to investigate the dynamics of submarine debris flows over three types of bed, including a mobile loose sand bed, an immobile smooth bed, an immobile rough bed. Details of the model setup and some preliminary findings are discussed in this conference paper.

RÉSUMÉ : Il a été signalé que les flux de débris sous-marins causaient de graves dommages aux infrastructures offshore, y compris les câbles, les pipelines et les plates-formes. Par rapport à leurs homologues subaériens, les flux de débris sous-marins ont généralement une échelle de plusieurs ordres de grandeur plus grande et parcourent une distance de faux-rond plus longue. Les flux de débris sous-marins sont souvent modélisés expérimentalement sur des lits rigides et imperméables. Cependant, en réalité, les fonds marins sont mobiles et perméables. Ces conditions de lit influencent l'échange de quantité de mouvement entre l'écoulement et le lit via des contraintes de frottement accrues, un drainage à l'interface lit d'écoulement et un échange de masse. Dans cette étude, un nouveau modèle de flux de débris sous-marins a été développé pour étudier la dynamique des flux de débris sous-marins sur trois types de lit, y compris un lit de sable mobile mobile, un lit lisse immobile, un lit rugueux immobile. Les détails de la configuration du modèle et quelques résultats préliminaires sont discutés dans ce document de conférence.

KEYWORDS: submarine debris flows; bed conditions; physical modelling.

1 INTRODUCTION

Submarine debris flows have been reported to cause damage to offshore infrastructure, including cables, pipelines, and platforms (Stevenson et al. 2018, Assier-Rzadkieaica et al. 2000). Compared to their subaerial counterparts, submarine debris flows are generally several orders of magnitude larger in scale and have a longer travel distance (Crandell et al. 1984, Nisbet & Piper 1998).

Given the poor temporal predictability of submarine debris flows, physical modelling is commonly used to elucidate their fundamental mechanisms (Mohrig et al. 1998, Ilstad et al. 2004b, Zakeri et al. 2008). The bulk of existing studies adopt immobile and impervious beds in their physical models (Mohrig et al. 1999, Harbitz et al. 2003). However, in reality the sea bed consists of loose sand (Bellec et al. 2009). Such bed conditions may affect the momentum exchange processes between the flow and bed via enhanced friction stresses, drainage at the flow-bed interface and entrainment (Iverson 2012).

Further compounding the challenges of modelling submarine debris flow is simulating hydroplaning. This phenomenon occurs when a clay-rich flow front is subjected to a high dynamic pressure, which causes the flow front to deform and uplift (Mohrig et al., 1998). Hydroplaning is widely reported to enhance the mobility of submarine debris flows (De Blasio et al., 2004). However, the effects of a mobile bed on hydroplaning have not yet to be elucidated. On one hand, a mobile loose sand bed may provide a drainage path to dissipate the excess pore pressures built-up underneath the flow front and reduce the effects of hydroplaning. On the other hand, a mobile loose sand bed may enhance the frictional stresses at the flow-bed interface, thereby decelerating the flow. The roles played by these competing effects on the flow dynamics of submarine debris flows remain poorly understood.

In this study, a new model was developed to investigate the dynamics of submarine debris flows over different bed conditions. Three types of beds were modelled, including a mobile loose sand bed, an immobile smooth bed, an immobile rough bed. Details of the new flume model are discussed and some preliminary results are presented.

2 MODEL SETUP

Figure 1 shows a photo of the new submarine debris flow model. The model consists of a gently-inclined tank at 18°. The tank is 3 m in length, 0.2 m in width, and 1 m in height at the downslope end and 0.5 m in height at the upslope end. A pneumatically controlled gate is installed near the upstream section of the tank to retain 0.02 m^3 of debris slurry. When the gate is opened, the inclined height of the opening between the gate and the channel bed is 0.25 m. The channel bed has a total length of about 1.8 m, which consists of three sections: a 0.8 m-long inclined section that is inclined at 18° to accelerate the flow; a curvilinear section that enables a smooth transition to a gently-inclined channel at 3°; and a gently-inclined section that has an overall length of about 0.8 m.

3 INSTRUMENTATION

A pore pressure transducer (model: AML Pi645LP100mBarg) was installed on the channel bed of the gently-inclined section (shown in Figure 1 and Figure 2) to measure the basal pore pressure changes of the flow. The transducer has a maximum measurement capacity of 101 kPa. The pore pressure transducer was installed before the bed section to ensure that the dynamics of the flows for each test were comparable before overriding different bed conditions. Other pore pressure transducers were installed in the mobile loose sand bed, but will not be discussed because they were not interpreted at the time of preparation of this conference paper.

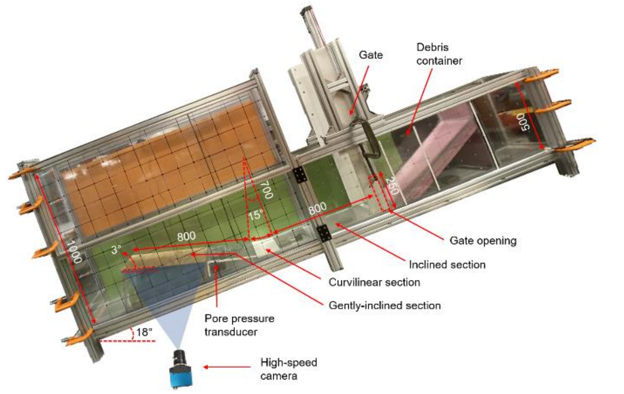

Figure 1. Schematic diagram showing the side view of submarine debris flow model with relevant instrumentations (all dimensions are in mm).

A high-speed camera (model: EcoSensmini2 MC3070) was installed at the side of the gently-inclined channel to capture the flow kinematics (shown in Figure 1). The velocity fields of the images were analysed using particle image velocimetry (Thielicke & Stamhuis 2014). The camera was set to capture images at a sampling rate of 300 frames per second with each image having a resolution of 1696 × 642 pixels.

4 SCALING

Two dimensionless numbers were considered to characterise the flows in this study. Specifically, the dimensionless yield number, τ_y^*, and the densimetric Froude number, Fr_d, respectively (Marr et al. 2001, Mohrig & Marr 2003, Ilsatd et al. 2004b, Liu et al. 2020):

$$\tau_y^* = \tau_y/\rho_w u^2 \quad (1)$$

$$Fr_d = u/\sqrt{(1-\rho_w/\rho_d)gH} \quad (2)$$

where τ_y is the flow yield strength, u is the frontal velocity, ρ_w is the density of water, ρ_d is the density of the debris material, and g is the gravitational acceleration. Eqn. 1 considers whether there is enough uplift force from the dynamic pressure and adequate yield strength of the flow to hydroplane. More specifically, the flow yield strength characterises the ability of a flow to remain coherent under the influence of dynamic pressure (Marr et al. 2001). Flows with a high yield strength typically have a high viscosity, which results in a low flow velocity. In turn, a low dynamic pressure is generated and the flow front is less likely to be lifted. The submarine debris flows can be characterised to be strongly coherent when $\tau_y^* > 0.1$ (Marr et al. 2001, Ilstad et al. 2004b). In this study, the measured τ_y^* for the modelled flows were only about 0.01.

Eqn. 2 is used to characterise the onset of hydroplaning. Based on the back-analyses of field data, densimetric Froude numbers were estimated to range from 0.2 to 2.5 (Mohrig et al. 1998, Talling et al. 2007, Stevenson et al. 2018). The experimental empirical threshold of the densimetric Froude number for hydroplaning is for values greater than 0.35 (Mohrig et al. 1998). In this study, the measured densimetric Froude numbers for the modelled flows were larger than 0.35. However, the low yield strength of the flows caused the front to be incoherent and hydroplaning was not observed.

5 TEST PLAN

Figure 2 shows the three different bed conditions that were modelled, specifically a mobile loose sand bed, an immobile smooth bed, and an immobile rough bed. For the mobile loose sand bed, the sand was prepared inside a container in the gently-inclined section to a target dry density of 1400 kg/m^3 to ensure the sand was in a loose state (Verdugo & Ishihara 1996). This bed consists of Toyoura sand with an estimated permeability of 10^{-12} m^2 (Danno & Kimura 2009). The container has dimensions of 0.5 m in length, 0.2 m in width and 0.1 m in depth at upslope side and 0.23 m in depth at downslope side. The sand was prepared in layers using the pluviation technique (Ueng et al. 2006) and then saturated (Zhai et al. 2018). For the immobile beds, impervious steel plates were used to cover the compartment where loose sand was prepared for the mobile bed. The immobile smooth bed was modelled using a metal plate with dimensions of 500 mm in length and 200 mm in width. For the immobile rough bed, a thin layer of Toyoura sand was attached on the metal plate using epoxy. The flow composition was kept the same for each test. Details of the flow composition will be discussed in the modelling procedures below.

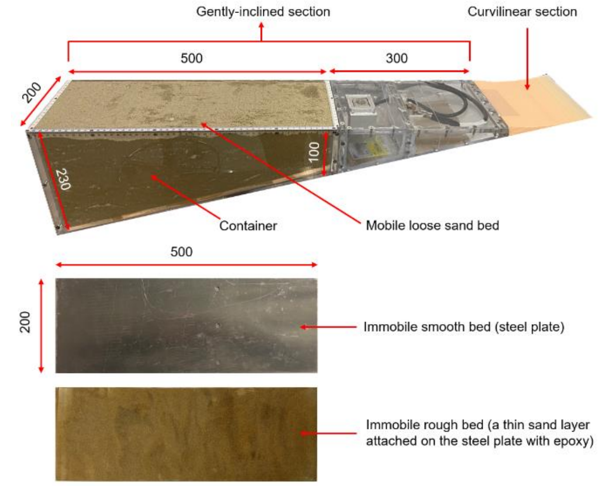

Figure 2. Schematic diagram of the curvilinear and gently-inclined sections where the bed conditions were varied. (all dimensions are in mm).

6 MODELLING PROCEDURES

Before each test, the appropriate bed conditions were prepared. The flume tank was inclined to 18° by using a hydraulic jack. The gently-inclined section used to model different bed conditions was then placed inside the tank. The gate was closed, and the tank was slowly filled with water. Afterwards, the debris mixture was prepared by mixing 4% of Kaolinite clay, 36% of Toyoura sand and 60% of water by volume. Toyoura sand has a mean diameter of 0.18 mm and the interface friction angle between the flow and bed is estimated to be 38° (Yoshimi et al. 1978, Ishihara 1993, Hatanaka & Uchida 1996). The specific gravity of Toyoura sand and Kaolinite clay are 2.65 and 2.70, respectively. The slurry was poured into the debris container. Before each test, the instrumentation was calibrated. The data logger and high-speed camera were triggered before opening the gate to allow the debris material to flow downslope.

7 OBSERVED AND MEASURED FLOW KINEMATICS

Figure 3 shows a typical snapshot taken from the mobile loose sand bed test with vectors overlaying the high-speed image. The flow moves towards the left. It can be observed that the vectors are laminar near the base and more random at the boundaries of the flow where turbidity currents form. This is consistent with results reported by Ilstad et al. (2004a).

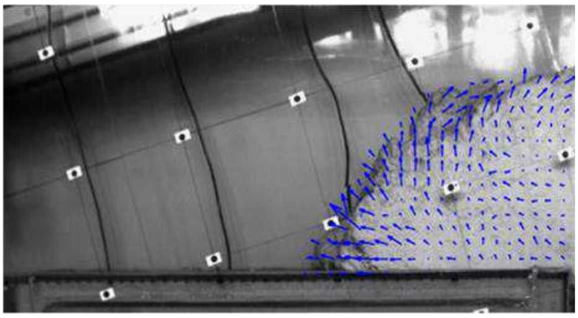

Figure 3. Snapshot of the flow kinematics for mobile loose sand bed test with vectors from particle image velocimetry.

Figure 4 shows a comparison of the frontal velocity profiles resulting from the different bed conditions modelled. The abscissa shows the frontal velocity and the ordinate shows the normalised distance along the mobile/immobile bed of the gently-inclined section. The velocity is observed to decrease for each test as the flow travels over the gently-inclined section. The frontal velocity of the flow on the immobile smooth bed exhibits the lowest velocity reduction of 16%. Some of the mobile bed surface is observed to be entrained, and the frontal velocity reduction of the flow on the mobile loose sand bed is 19%. The frontal velocity reduction of the flow on the immobile rough bed exhibits the highest frontal velocity reduction of 22%.

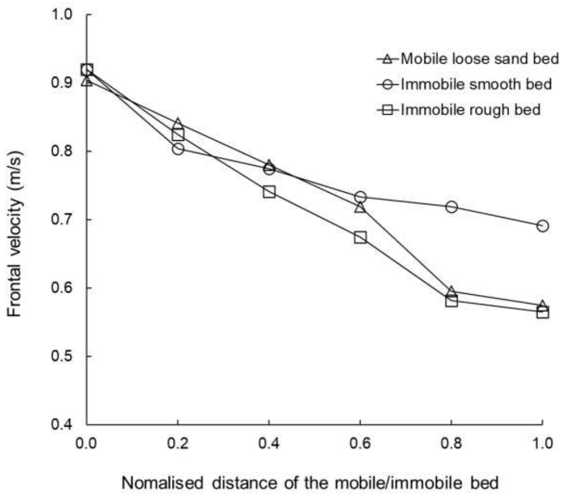

Figure 4. Comparison of frontal velocity profiles of the flow on different bed conditions.

The comparison of the frontal velocities indicates that bed roughness plays an important role in the flow kinematics. Moreover, roughening an immobile bed may not realistically capture the kinematics of a flow on a loose sand bed.

8 SUMMARY

Details of a new submarine debris flow model are described. The physical data from this model can be used to reveal fundamental mechanisms of the interaction between submarine debris flows over different bed conditions. Furthermore, high quality and systematic experimental data can be used to understand scale effects and calibrate numerical models for the numerical back-analysis and parametric studies.

9 ACKNOWLEDGEMENTS

The authors are grateful for the generous financial sponsorship from the National Natural Science Foundation of China (51709052), as well as the Research Grants Council of Hong Kong (General Research Fund Grants 16212618; 16209717; 16210219; T22-603/15N; AoE/E-603/18).

10 REFERENCES

Assier-Rzadkieaicz, S., Heinrich, P., Sabatier, P. C., Savoye, B., & Bourillet, J. F. (2000). Numerical modelling of a landslide-generated tsunami: the 1979 Nice event. *Pure and Applied Geophysics*, *157*(10), 1707-1727.

Bellec, V. K., Dolan, M. F., Bøe, R., Thorsnes, T., Rise, L., Buhl-Mortensen, L., & Buhl-Mortensen, P. (2009). Sediment distribution and seabed processes in the Troms II area-offshore North Norway. *Norwegian Journal of Geology/Norsk Geologisk Forening*, *89*.

Crandell, D. R., Miller, C. D., Glicken, H. X., Christiansen, R. L., & Newhall, C. G. (1984). Catastrophic debris avalanche from ancestral Mount Shasta volcano, California. *Geology*, *12*(3), 143-146.

Danno, K., & Kimura, M. (2009). Evaluation of long-term displacements of pile foundation using coupled FEM and centrifuge model test. *Soils and Foundations*, 49(6), 941-958.

De Blasio, F. V., Engvik, L., Harbitz, C. B., & Elverhøi, A. (2004). Hydroplaning and submarine debris flows. *Journal of Geophysical Research: Oceans*, *109*(C1).

Harbitz, C. B., Parker, G., Elverhøi, A., Marr, J. G., Mohrig, D., & Harff, P. A. (2003). Hydroplaning of subaqueous debris flows and glide blocks: Analytical solutions and discussion. *Journal of Geophysical Research: Solid Earth*, *108*(B7).

Hatanaka, M., & Uchida, A. (1996). Empirical correlation between penetration resistance and internal friction angle of sandy soils. *Soils and foundations*, *36*(4), 1-9.

Ilstad, T., Elverhøi, A., Issler, D., & Marr, J. G. (2004a). Subaqueous debris flow behaviour and its dependence on the sand/clay ratio: a laboratory study using particle tracking. *Marine Geology*, *213*(1-4), 415-438.

Ilstad, T., Marr, J. G., Elverhøi, A., & Harbitz, C. B. (2004b). Laboratory studies of subaqueous debris flows by measurements of pore-fluid pressure and total stress. *Marine Geology*, *213*(1-4), 403-414.

Ishihara, K. (1993). Liquefaction and flow failure during earthquakes. *Geotechnique*, *43*(3), 351-451.

Iverson, R. M. (2012). Elementary theory of bed-sediment entrainment by debris flows and avalanches. *Journal of Geophysical Research: Earth Surface*, *117*(F3).

Liu, D., Cui, Y., Guo, J., Yu, Z., Chan, D., & Lei, M. (2020). Investigating the effects of clay/sand content on depositional mechanisms of submarine debris flows through physical and numerical modeling. *Landslides*, *17*(8), 1863-1880.

Marr, J. G., Harff, P. A., Shanmugam, G., & Parker, G. (2001). Experiments on subaqueous sandy gravity flows: The role of clay and water content in flow dynamics and depositional structures. *Geological Society of America Bulletin*, *113*(11), 1377-1386.

Mohrig, D., & Marr, J. G. (2003). Constraining the efficiency of turbidity current generation from submarine debris flows and slides using laboratory experiments. *Marine and Petroleum Geology*, *20*(6-8), 883-899.

Mohrig, D., Ellis, C., Parker, G., Whipple, K. X., & Hondzo, M. (1998). Hydroplaning of subaqueous debris flows. *Geological Society of America Bulletin*, *110*(3), 387-394.

Mohrig, D., Elverhøi, A., & Parker, G. (1999). Experiments on the relative mobility of muddy subaqueous and subaerial debris flows, and their capacity to remobilize antecedent deposits. *Marine Geology*, *154*(1-4), 117-129.

Nisbet, E. G., & Piper, D. J. (1998). Giant submarine landslides. *Nature*, *392*(6674), 329-330.

Stevenson, C. J., Feldens, P., Georgiopoulou, A., Schönke, M., Krastel, S., Piper, D. J., Lindhorst, K. & Mosher, D. (2018). Reconstructing the sediment concentration of a giant submarine gravity flow. *Nature communications*, 9(1), 1-7.

Talling, P. J., Wynn, R. B., Masson, D. G., Frenz, M., Cronin, B. T., Schiebel, R., ... & Georgiopoulou, A. (2007). Onset of submarine debris flow deposition far from original giant landslide. *Nature*, *450*(7169), 541-544.

Thielicke, W., & Stamhuis, E. (2014). PIVlab–towards user-friendly, affordable and accurate digital particle image velocimetry in MATLAB. *Journal of open research software*, *2*(1).

Ueng, T. S., Wang, M. H., Chen, M. H., Chen, C. H., & Peng, L. H. (2006). A large biaxial shear box for shaking table test on saturated sand. *Geotechnical Testing Journal*, *29*(1), 1-8.
Verdugo, R., & Ishihara, K. (1996). The steady state of sandy soils. *Soils and foundations*, *36*(2), 81-91.
Yoshimi, Y., Hatanaka, M., & Oh-Oka, H. I. R. O. S. H. I. (1978). Undisturbed sampling of saturated sands by freezing. *Soils and Foundations*, *18*(3), 59-73.
Zakeri, A., Høeg, K., & Nadim, F. (2008). Submarine debris flow impact on pipelines-Part I: Experimental investigation. *Coastal engineering*, *55*(12), 1209-1218.
Zhai, Y., He, R., Zhao, J., Zhang, J., Jeng, D. S., & Li, L. (2018). Physical model of wave-induced seabed response around trenched pipeline in sandy seabed. *Applied Ocean Research*, *75*, 37-52.